SLEEPJ, 2021, 1–13

doi: 10.1093/sleep/zsaa286
Advance Access Publication Date: 22 December 2020
Original Article

ORIGINAL ARTICLE

Complement promotes endothelial von Willebrand factor and angiopoietin-2 release in obstructive sleep apnea

Su Gao[1,†], Memet Emin[1,†], Theodosia Thoma[1], Kalliopi Pastellas[1], Francesco Castagna[1,], Riddhi Shah[1], Alondra Jimenez[1], Neha Patel[1], Ying Wei[2] and Sanja Jelic[1,*]

[1]Division of Pulmonary, Allergy, and Critical Care Medicine and [2]Division of Biostatistics, Columbia University College of Physicians and Surgeons, New York, NY

[†]These authors are equal first authors to this work.

*Corresponding author. Sanja Jelic, Columbia University College of Physicians and Surgeons, Division of Pulmonary, Allergy, and Critical Care Medicine, 630 West 168th Street, PH8 Center, Room 101, New York, NY 10032. Email: sj366@cumc.columbia.edu

Abstract

Study Objective: Obstructive sleep apnea (OSA) is highly prevalent and triples vascular thromboembolic risk. Intermittent hypoxia (IH) during transient cessation of breathing in OSA impairs endothelial protection against complement. Complement activation stimulates the endothelial release of a pro-thrombotic von Willebrand factor (vWF). We investigated whether increased complement activity in OSA promotes the endothelial release of vWF and pro-inflammatory angiopoietin-2. We further investigated whether improving complement protection with statins reverses these changes.

Methods: Using endothelial cells (ECs) and blood collected from OSA patients (n = 109) and controls (n = 67), we assessed whether altered cellular localization of complement inhibitor CD59 in OSA modulates exocytosis of Weibel-Palade bodies (WPB), secretory granules that store vWF and angiopoietin-2. These interactions were also assessed in vitro in ECs exposed to normoxia or IH with or without recombinant complement C9 and with or without atorvastatin.

Results: Circulating levels of angiopoietin-2 were greater in OSA than controls and levels of vWF cleavage products correlated with OSA severity. In cultured ECs, IH enhanced complement-stimulated angiopoietin-2 and vWF release by reducing EC surface and increasing intracellular expression of complement inhibitor CD59. Intracellular CD59 co-localized with WPB in OSA. IH increased binding of intracellular CD59 to syntaxin-3, which dissociated syntaxin-3 from voltage-sensitive calcium channel $Ca_v1.2$, and activated WPB exocytosis in a calcium-dependent manner. Atorvastatin reversed IH-enhanced endothelial release of vWF and angiopoietin-2.

Conclusions: IH promotes the complement-mediated release of vWF and angiopoietin-2, which may contribute to pro-thrombotic and pro-inflammatory conditions in OSA. Statin reversed these effects, suggesting a potential approach to reduce cardiovascular risk in OSA.

Statement of Significance

Impaired endothelial complement inhibition in obstructive sleep apnea promotes the release of pro-thrombotic von Willebrand factor and pro-inflammatory angiopoietin-2. Statins reversed these effects in a CD59-dependent manner in intermittent hypoxia, suggesting a possible therapeutic strategy to reduce cardiovascular risk in obstructive sleep apnea that may be complementary to continuous positive airway pressure and/or particularly useful in obstructive sleep apnea patients who do not adhere to continuous positive airway pressure.

Key words: obstructive sleep apnea; endothelium; complement; von Willebrand factor; angiopoietin-2; Weibel-Palade bodies

Submitted: 18 September, 2020; **Revised:** 3 November, 2020

Introduction

Obstructive sleep apnea (OSA) affects a quarter of Western adults and triples the risk for cardiovascular disease, including hypertension, coronary artery disease, stroke, and venous thromboembolism [1, 2]. Intermittent hypoxia (IH) during transient cessation of breathing in OSA leads to endothelial activation, a key step in the initiation and progression of cardiovascular disease [3–5]. However, the mechanisms that mediate IH-induced endothelial activation are incompletely understood and no targeted therapy is available for IH-induced vascular alterations in OSA. In addition, standard therapy for OSA with continuous positive airway pressure (CPAP) does not reduce cardiovascular risk in randomized clinical trials, further highlighting the need for alternative therapies for OSA-related cardiovascular disease [6–8].

We reported recently that IH promotes internalization of a major complement inhibitor CD59 from the endothelial cell (EC) surface resulting in increased complement activity and inflammation in OSA patients—a cholesterol-dependent process that is reversed by statins [5]. Complement activation stimulates the rapid release of a pro-thrombotic multimer von Willebrand factor (vWF) from ECs [9–11]. vWF plays important role in arterial and venous thrombosis and atherosclerosis—conditions strongly associated with OSA [2, 12–15]. In ECs, vWF is stored in Weibel-Palade bodies (WPB), secretory granules that also contain angiopoietin-2, a cytokine that destabilizes endothelial integrity and promotes vascular inflammation [16, 17]. Interestingly, circulating levels of angiopoietin-2 correlate inversely with oxygen levels during sleep; however, the underlying mechanisms are unclear [18]. Considering that IH promotes endothelial complement activation and inflammation in OSA and that complement activation stimulates the endothelial release of vWF, we investigated whether IH modulates vWF and angiopoietin-2 release from WPB via complement activation in OSA. We also investigated whether these interactions could be targeted therapeutically by statins to reduce pro-thrombotic and pro-inflammatory conditions that contribute to cardiovascular risk in patients with OSA.

Methods

Study participants and design

We prospectively recruited participants from the Sleep Center at Columbia University. All study participants underwent nocturnal polysomnography. An apnea–hypopnea index (AHI) greater than or equal to 5 obstructive events per hour of sleep established the diagnosis of OSA. Study participants with AHI less than 5 events/h were considered OSA-free. All patients with suspected sleep-disordered breathing who were referred for nocturnal polysomnography were screened. Patients with coronary artery disease, heart failure, a history of stroke, diabetes mellitus, chronic obstructive or restrictive pulmonary disease, chronic kidney disease, dyslipidemia, hypertension requiring more than one medication or tobacco use within the past 10 years were ineligible for the study. Nocturnal polysomnography was performed with an Embla signal recording system and Somnologica Window NT Software (Flaga Group hf. Medical Devices). Sleep stages were scored in 30-s epochs according to standard criteria. An obstructive apnea was defined as a cessation of upper airway flow in association with continued respiratory effort of at least 10 s. An obstructive hypopnea was defined as a discrete reduction in airflow associated with a decrease in oxygen saturation of 3% or more for at least 10 sin the presence of thoracoabdominal ventilatory efforts. AHI was defined as the number of obstructive apnea plus hypopnea episodes per hour of sleep. An oxygen desaturation index (ODI) was defined as the number of greater than or equal to 3% arterial oxygen desaturations per hour of sleep. Daytime sleepiness was assessed by Epworth Sleepiness Scale (0–9 normal sleepiness, 10–24 increased sleepiness). EC harvesting was performed between 9:00 and 11:00 am after polysomnography while study participants were in a fasting state. In two OSA patients who underwent split-night polysomnography with CPAP titration [19], harvesting was performed 48 h later to avoid any CPAP interference. According to the American Academy of Sleep Medicine Clinical Practice Guideline, a split-night protocol was performed when the following criteria were met: (1) a moderate to severe degree of OSA is observed during a minimum of 2 h of recording time on the diagnostic PSG, and (2) at least 3 h are available for CPAP titration. The Columbia University institutional review board approved the study. All study participants gave written informed consent.

EC harvesting and isolation

ECs harvesting from participants was performed as described previously [5]. Briefly, a 20-gauge angiocatheter was inserted into the superficial forearm vein under sterile conditions. Next, three J-shaped vascular guide wires (Arrow) were sequentially advanced into the vein up to 10 cm while maintaining sterile conditions. ECs were collected from wire tips by washing with EC dissociation buffer. For immunofluorescence, ECs were recovered by centrifugation at 4°C, 150 g for 6 min and resuspended in red blood cell (RBC) lysis buffer (155 mM NH_4Cl, 10 mM $KHCO_3$, 0.1 mM EDTA). The suspension was incubated at 4°C for 5 min, centrifuged at 150 g for 6 min, fixed with 4% paraformaldehyde (Alfa Aesar) in phosphate-buffered saline (PBS) for 10 min, washed twice with PBS, transferred to poly-l-lysine–coated slides (Electron Microscopy Sciences) and air-dried at 37°C. For RNA extraction, the ECs were isolated using biotinylated mouse anti-human antibody against CD146 (Millipore), and Streptavidin FlowComp Dynabeads (Invitrogen) at 4°C for 45 min followed by magnet isolation.

Assessment of plasma VWF levels

Deidentified plasma samples from OSA patients and controls were centrifuged and frozen in –80° until being analyzed in the commercial laboratory (ARUP Laboratories, Salt Lake City, Utah) as described in detail in Supplemental Material.

Cell culture

Human umbilical venous ECs (HUVECs) (BD Biosciences) were cultured in EC medium with 2% endotoxin-free heat-inactivated fetal bovine serum (Life Technologies) until they reached the required confluence for each experiment. For complement-stimulation experiments, recombinant C9 0.1 μg/cm^2 cells (Abnova) was added to heat-inactivated serum. For calcium

chelation experiments, BAPTA (Life Technologies) was dissolved in DMSO (0.1% in the medium) and 25 μM was used in the culture medium. For atorvastatin experiments, HUVECs were incubated with heat-inactivated serum (with or without recombinant C9 as detailed for each experiment) with or without the addition of 1 μM atorvastatin (Sigma–Aldrich) dissolved in DMSO (0.01% in the medium) for 8 h in normoxia or IH. Passages 3–6 were used for all experiments.

Intermittent hypoxia

A hypoxia chamber (BioSpherix) housed inside an incubator kept at 37°C was used or all IH experiments. HUVECs subjected to IH were exposed to 21% O_2 with 5% CO_2 for normoxia and 2% O_2 with 5% CO_2 for hypoxia for alternating 30-min cycles for a total exposure time of 8 h [5].

Immunofluorescence

Harvested ECs were identified on slides by positive staining with goat anti-human VE-Cadherin (R&D system), followed by FITC-conjugated donkey anti-goat secondary antibody (Jackson Immunology). HUVECs were fixed with 4% paraformaldehyde. Cell nuclei were stained with 4′, 6-diamidino-2-phenylindole (DAPI; Life Technologies).

CD59-vWF co-localization by proximity ligation assay (Duolink): Fixed ECs collected from participants or HUVECs were permeabilized, and incubated with rabbit anti-CD59 and mouse anti-vWF antibody using Duolink in situ kit (Sigma). EC plasma membrane was identified by goat anti-VE-Cadherin (R&D System) followed by FITC-conjugated donkey anti-goat secondary antibody. Nucleus was stained by DAPI (Life Technologies). CD59-vWF co-localization was expressed as fluorescence area (μm^2). Confocal microscopy (Nikon Instruments Inc.) and Image J were used for analysis.

Intracellular vWF expression in HUVECs: HUVECs were permeabilized with 0.2% Triton X-100 for 10 min and blocked with 5% BSA for 30 min, incubated with mouse anti-vWF (Abcam) and goat anti-VE-Cadherin followed by FITC-conjugated donkey anti-mouse (Jackson Immunology) and Alexa 633-conjugated donkey anti-goat (Life Technologies) at room temperature for 30 min. Nucleus was stained by DAPI. Expression of intracellular vWF was expressed as fluorescence area (μm^2).

CD59 and MAC in ECs from participants: For assessment of cellular distribution of CD59, harvested ECs were identified by positive staining with goat anti-human polyclonal antibodies directed against VE-cadherin (R&D Systems) followed by FITC-conjugated donkey anti-goat secondary antibodies (Jackson ImmunoResearch). CD59 expression was assessed with rabbit anti-human antibodies directed against CD59 (Abcam) followed by Texas Red–conjugated donkey anti-rabbit secondary antibodies (Jackson ImmunoResearch). ImageJ was used to draw two lines along the EC plasma membrane, which was defined as the area with positive staining for VE-cadherin. The inner line was drawn along the interior border of VE-cadherin–positive area, and the outer line was drawn along the exterior border of VE-cadherin–positive area. The fluorescence intensity of the CD59-positive area between two lines was quantified (μm^2) and represented EC surface CD59 expression. The fluorescence intensity of the CD59-positive area in each EC located within an outer line represented total EC CD59 expression (μm^2). The ratio of the CD59-positive area between two lines divided by the CD59-positive area located within an outer line (total EC CD59 expression) represented the proportion of CD59 located on the EC surface [5]. A minimum of 10 (range 10–30) consecutive ECs were analyzed for each slide. Investigators who analyzed the slides were blinded to the OSA status of the study participants.

For assessment of MAC deposition on harvested ECs, unpermeabilized harvested ECs were identified by positive staining with goat anti-human polyclonal antibodies directed against VE-cadherin (R&D Systems), followed by FITC-conjugated donkey anti-goat secondary antibodies (Jackson ImmunoResearch). MAC deposition was assessed with mouse anti-human monoclonal antibodies directed against C5b-9 (MAC) (clone aE11, DAKO), followed by Texas Red–conjugated donkey anti-mouse secondary antibodies (Jackson ImmunoResearch). All immunofluorescence data were analyzed with confocal microscopy (Nikon Instruments Inc.) and Image J.

Flow cytometry

For quantification of the EC surface vWF expression, we used flow cytometry and HUVECs. After 8 h exposure to IH or normoxia, HUVECs were dissociated from culture plate by TrypLE Express cell-dissociation enzymes (Thermo Fisher) and placed on ice. Non-permeabilized HUVECs were incubated with Alexa 488-conjugated rabbit anti-human vWF (Abcam) at 4°C for 1 h and analyzed using FACS Canto cytometer (BD Biosciences). Alexa 488-conjugated non-specific Rabbit IgG (Abcam) was used as negative control.

Enzyme-linked immunosorbent assay

Human vWF SimpleStep ELISA Kit (Abcam) and Human Angiopoietin-2 ELISA Kit (Millipore) were used to determine the level of vWF and angiopoietin-2 in the HUVEC culture media according to the manufacturer's protocol.

CD59 siRNA treatment

Small interfering (si)RNA treatment was carried out with DharmaFECT transfection reagent (Dharmacon) for 48 h according to the manufacturer's protocol using 50 nM oligonucleotides (ON-TARGETplus Human CD59 (966) siRNA–SMARTpool). Using Western blotting, we confirmed that CD59 (966) siRNA reduced CD59 protein expression by greater than 90% (Supplementary material Figure S4). Scrambled RNA was used as a negative control.

Immunoprecipitation and Western blotting

After exposure to normoxia or IH, HUVEC lysate was incubated with antibodies for vWF (Abcam), syntaxin-3 (Synaptic Systems or Santa Cruz Biotechnology), vesicle-associated membrane protein (VAMP) 3 (Cell Signaling Technology) or VAMP8 (Novus Biologicals) overnight at 4°C. To detect possible interaction between intracellular CD59 and syntaxin-3, HUVECs were treated with cell-permeable crosslinking solution of 2 mM 3,3-Dithiodipropionic acid di(N-hydroxysuccinimide ester) (DSP)

(Sigma) for 15 min under room temperature prior to lysis after exposure to normoxia or IH. For co-immunoprecipitation of syntaxin-3 and $Ca_v1.2$ or $Ca_v3.1$, HUVECs were incubated with 1 mM DSP for 30 min under room temperature before prior to lysis. Agarose suspension (Cell Signaling Technology) was added and the mixture was incubated overnight at 4°C. The immune complex was precipitated by centrifugation for 5 min at 1000 g at 4°C. The pellet was washed and re-suspended in Laemmli sample buffer containing β-mercaptoethanol, boiled for 5 min and centrifuged. The supernatant was loaded to gels. In Western blotting, HUVECs were lysed on ice with cell lysis buffer (Cell Signaling Technology) supplemented with Pierce protease and phosphatase inhibitor (ThermoScientific). Protein amount in the lysate was determined by Pierce BCA protein assay (ThermoScientific) to ensure equal protein loading on gels. Protein samples were mixed with Laemmli Sample Buffer (BIO-RAD) and separated on PROTEAN TGX Precast Protein Gel (BIO-RAD). Standard immunoblotting procedure was performed based on the manufacturer's instructions (BIO-RAD). Primary antibodies for CD59 (R&D Systems), vWF (Abcam), syntaxin-3 (Abcam), VAMP3 and VAMP8 (Novus Biologicals), $Ca_v1.2$ and $Ca_v3.1$ (Abcam) were used.

Quantitative real-time PCR

RNA from HUVECs was extracted with TRIzol reagent (Ambion). Reverse transcription reaction was performed with qSCRIPT XLT cDNA Supermix (Quanta Bio). For a 20 μL of real-time PCR assay, the following reagents were added: 10 μL of TaqMan Gene Expression Master Mix (2X) (ThermoScientific), 1 μL of TaqMan primers and probe for detecting vWF (20X), 5 μL of nuclease-fee water, and 4 μL of cDNA. This reaction mixture was added to the wells as duplicates for each sample. Results were expressed as C_t values normalized to the reference gene β-actin.

Statistical analysis

Results are presented as mean ± standard error (SE; in vitro data), mean ± standard deviation (SD; data from participants) or percentage (%), as appropriate. The baseline characteristics of OSA patients and control subjects are expressed as the group-specific summary statistics, including age, gender, body-mass index (BMI), arterial oxyhemoglobin saturation (SaO_2) nadir, AHI, ODI, time spent below SaO_2 of 90% during sleep ($t < 90\%$), Epworth Sleepiness Scale, systolic and diastolic blood pressure, and physician-confirmed diagnosis of hypertension. Whether baseline characteristics significantly differ between the two groups was formally tested by a two-sample *t*-test (for continuous variables) or chi-square test (for binary variables). Owing to a relatively small sample size and non-normal distributions, the Exact permutation test was used to determine whether the mean outcomes are significantly different between OSA patients and controls. A linear model for each outcome was constructed, with OSA status as the primary predictor and age, gender, BMI, hypertension, systolic, and diastolic blood pressure as covariates. We used linear models to evaluate whether these covariates are associated with the outcome and whether the observed differences between OSA patients and controls are confounded by these covariates. To further adjust for potential confounders, we use backward Akaike information criterion to determine the optimal regression model. We started with a full model that includes AHI and all the potential confounders as covariates. We then dropped the most insignificant confounders, one at a time, until the AIC reached minimal values. The final model for each outcome is reported with specific potential confounders stated in the corresponding figure legends. *p* Values of less than 0.05 indicate statistical significance. No statistical method was used to predetermine the sample size. There was no pre-specified effect size in this prospective study. Post hoc power analysis showed that when statistical significance was reported for human samples, the probability of rejecting the null hypothesis was greater than 90%. For in vitro experiments, a two-sided *t*-test was used for all comparisons.

Results

Circulating levels of angiopoietin-2 and vWF cleavage products are increased in OSA patients

Circulating angiopoietin-2 and vWF multimers originate from WPB in ECs. To assess whether OSA modulates WPB exocytosis, we first quantified circulating levels of vWF and angiopoietin-2 in patients with OSA and OSA-free controls. Demographic characteristics of the participants are depicted in Supplementary material Table S1. Circulating levels of angiopoietin-2 were greater in OSA patients compared with controls (Figure 1, A), suggesting that OSA is associated with augmented secretion of angiopoietin-2 from WPB. To assess whether the difference between OSA and controls is driven by outlier values, we also performed comparison without outliers and the difference remained significant ($p = 0.03$, permutation test). Angiopoietin-2 levels did not correlate with severity of OSA as assessed by AHI, ODI or $t < SaO_2$ 90% ($r^2 = 0.0144$, –1e–04 and 0.0036, respectively; p = NS for all). Although age and BMI differ between OSA patients and controls, they were not associated with angiopoietin-2 levels and are unlikely to be a confounder (Supplementary material Table S2). Initially secreted as ultra-large molecular weight multimers, vWF is then cleaved by a disintegrin and metalloproteinase with a thrombospondin type 1 motif member 13 (ADAMTS13) into high (HMW), intermediate (IMW), and low molecular weight (LMW) multimers. There was a trend to increased LMW multimer level in plasma in OSA that did not reach significance (Supplementary material Figure S1) possibly reflecting many variables that affect these levels [20]. However, circulating levels of both IMW (adjusted for gender and DBP) and LMW (adjusted for BMI) multimers correlated positively with the severity of OSA as assessed by AHI (Figure 1, B and C and Supplementary material Tables S3–S5), suggesting that OSA is associated with augmented secretion of vWF from WPB. Furthermore, circulating LMW levels correlated positively with ODI and $t < 90\%$, indicators of the severity of repetitive hypoxemia in OSA patients (Figure 1, C), suggesting that IH promotes vWF release in OSA patients.

IH promotes endothelial vWF secretion in a complement-dependent manner

Terminal complement membrane attack complex (MAC) deposition on the surface of human umbilical vein endothelial cells

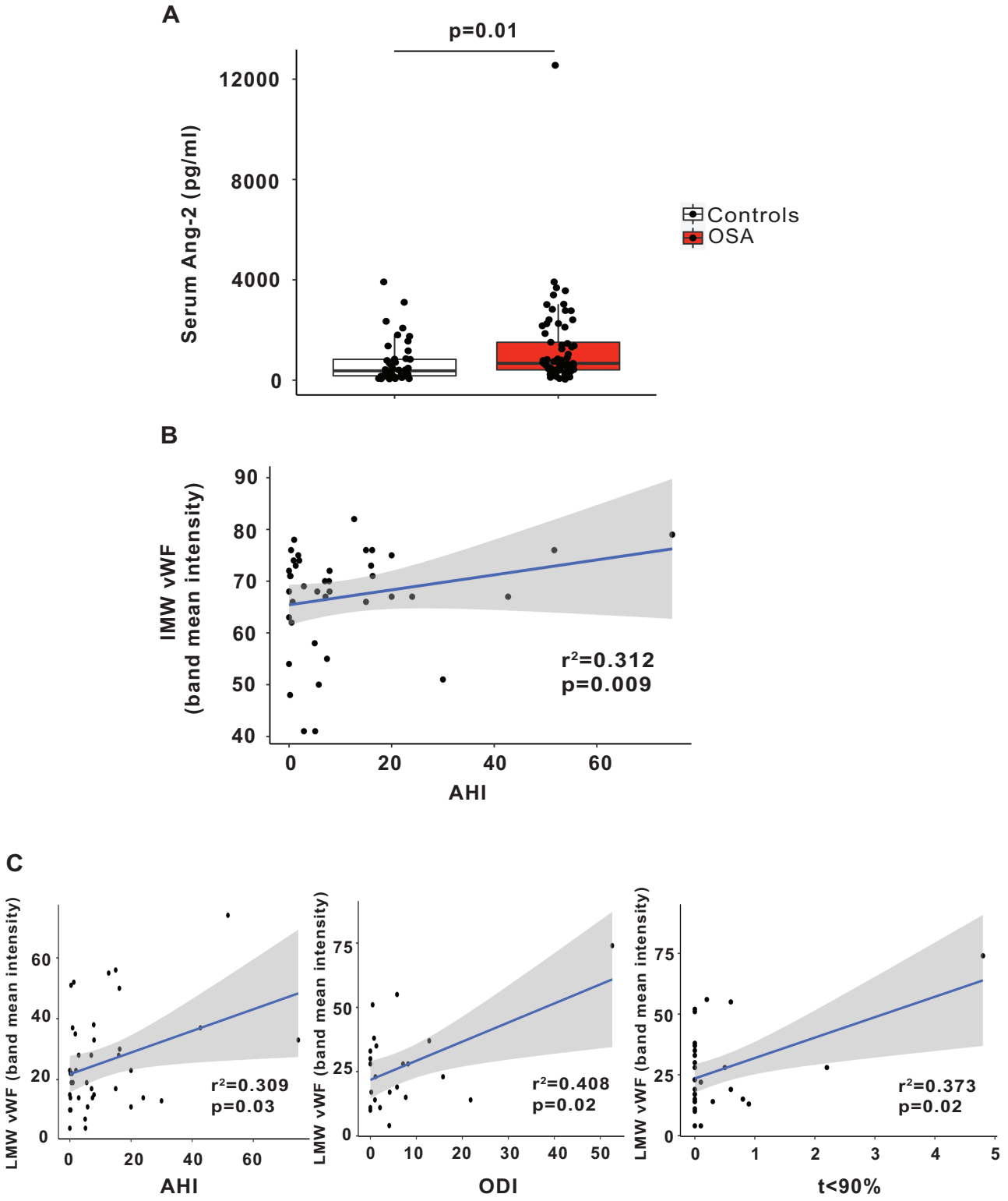

Figure 1. Increased levels of angiopoietin-2 and the association of vWF cleavage products with severity of OSA. (A) Quantitation of serum angiopoietin-2 levels from OSA patients (n = 69) and controls (n = 44) expressed as pg/mL (mean ± SD, permutation test). (B) Correlation of IMW vWF multimers with AHI adjusted for gender and diastolic blood pressure (n = 22 OSA patients and n = 18 controls). (C) Correlation of LMW vWF multimers with AHI, ODI and t < 90% (permutation test adjusted for BMI). AHI, apnea–hypopnea index; Ang-2, angiopoietin-2; BMI, body mass index; IMW, intermediate molecular weight; LMW, low molecular weight; ODI, oxygen desaturation index; OSA, obstructive sleep apnea; vWF, von Willebrand factor; t < 90% = time spent below oxyhemoglobin saturation of 90% during sleep.

(HUVECs) is known to stimulate rapid secretion of vWF [9]. MAC deposition was increased whereas the proportion of the total cellular complement inhibitor CD59 on the EC surface was reduced in ECs harvested from untreated OSA patients compared with controls, suggesting increased complement activity in OSA (Supplementary material Figure S2A and B). This prompted us to investigate whether IH modulates vWF release from ECs via complement activity.

We quantified endothelial vWF release after complement stimulation in IH. Whole serum, which is often used as a source of complement components, contains a variable concentration of vWF thereby precluding quantitation of vWF release from ECs. Therefore, we used recombinant human C9 protein that has pore-formation ability and intracellular signaling effect analogous to MAC [21, 22]. We incubated HUVECs with recombinant human C9 and quantified vWF released into the culture media. The levels of vWF in the culture media were similar in normoxia and IH (Figure 2, A). However, the intracellular vWF protein expression was markedly decreased in IH compared with normoxia after exposure to C9 (Figure 2, B and C), suggesting that IH does promote the release of vWF from WPB. We then investigated the possibility that vWF is retained on the cell surface after C9-stimulated release. Indeed, the cell surface expression of vWF was significantly greater in IH compared with normoxia (Figure 2, D and E). Thus, IH enhances complement-mediated release of vWF from WPB, and the released vWF predominantly adheres to the EC surface.

We then assessed whether IH modulates the release of vWF from WPB independently from complement activity. In the absence of complement (HUVECs incubated with heat-inactivated serum that is free of complement components), IH did not induce the release of vWF into the culture media (Supplementary material Figure S3A) or its expression on the EC surface (Supplementary material Figure S3B). In fact, IH increased expression of vWF intracellular protein (Supplementary material Figure S3C) likely owing to slightly upregulated vWF mRNA expression (a non-significant trend, $p = 0.07$) compared with normoxia (Supplementary material Figure S3D). These data show that complement is required for vWF release in IH.

To investigate whether CD59 modulates complement-stimulated vWF release from ECs in IH, we silenced the expression of CD59 in HUVECs using small interfering RNA (siRNA) (Supplementary material Figure S4) [5]. HUVECs with CD59 knockdown were incubated with C9 and exposed to normoxia or IH. CD59 knockdown increased the release of vWF compared with control in both normoxia and IH (Figure 3, A). CD59 did not alter vWF expression on the EC surface compared with control in both normoxia and IH (Figure 3, B and C).

IH-induced release of angiopoietin-2 from WPB is complement-dependent

The release of angiopoietin-2 from WPB parallels the release of vWF [17]. We investigated whether IH modulates the

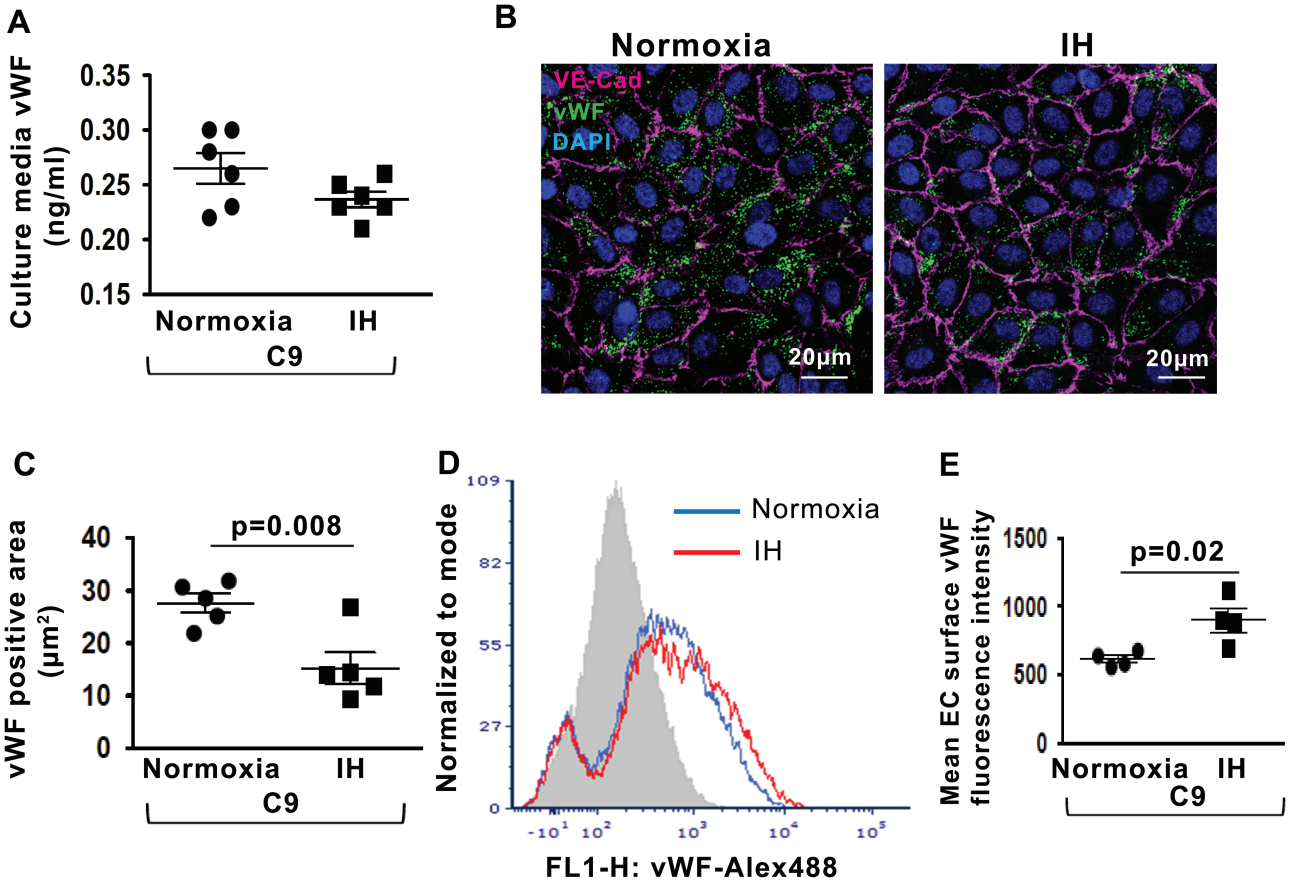

Figure 2. IH enhances complement-mediated release of endothelial vWF. (A) Quantitation of vWF levels in HUVEC culture media in normoxia and IH after stimulation with recombinant C9 expressed in ng/mL ($n = 6$). (B) Representative confocal images of intracellular vWF protein expression in HUVECs after stimulation with C9 in normoxia and IH. EC plasma membrane is identified by immunofluorescence for Vascular Endothelial (VE)–cadherin. Scale bar: 20 µm. (C) Quantitation of intracellular vWF protein expression levels (fluorescence area in µm²) in HUVECs after stimulation with C9 in normoxia and IH ($n = 5$). (D) Representative histogram with a log scale x-axis of vWF fluorescence intensity on the cell surface in HUVECs after stimulation with C9 in normoxia and IH. (E) Quantitation of vWF expression levels on the cell surface in HUVECs after stimulation with C9 in normoxia and IH expressed as mean fluorescence intensity ($n = 4$). All data throughout the figure are shown as the mean ± SE, two-sided *t*-test test. EC, endothelial cell; HUVECs, Human Umbilical Vein Endothelial Cells; IH, intermittent hypoxia; vWF, von Willebrand factor.

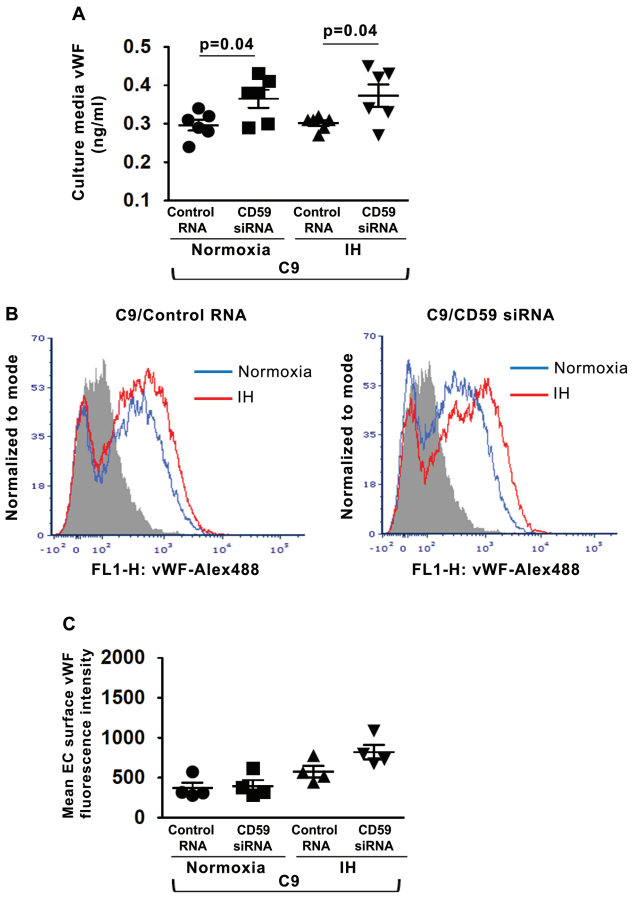

Figure 3. CD59 modulates complement-stimulated vWF release from ECs. (A) Quantitation of vWF levels in HUVECs culture media in normoxia and IH after stimulation with recombinant C9 and transfection with CD59 siRNA or control RNA (ng/mL) (n = 6). (B) Representative histogram with a log scale x-axis of vWF fluorescence intensity on the cell surface in HUVECs in normoxia and IH after stimulation with C9 and transfection with CD59 siRNA or control RNA. (C) Quantitation of vWF expression on the cell surface in HUVECs after stimulation with C9 in normoxia and IH expressed as mean fluorescence intensity (n = 4). All data throughout the figure are shown as the mean ± SE two-sided t-test test. Abbreviations as in Figure 2.

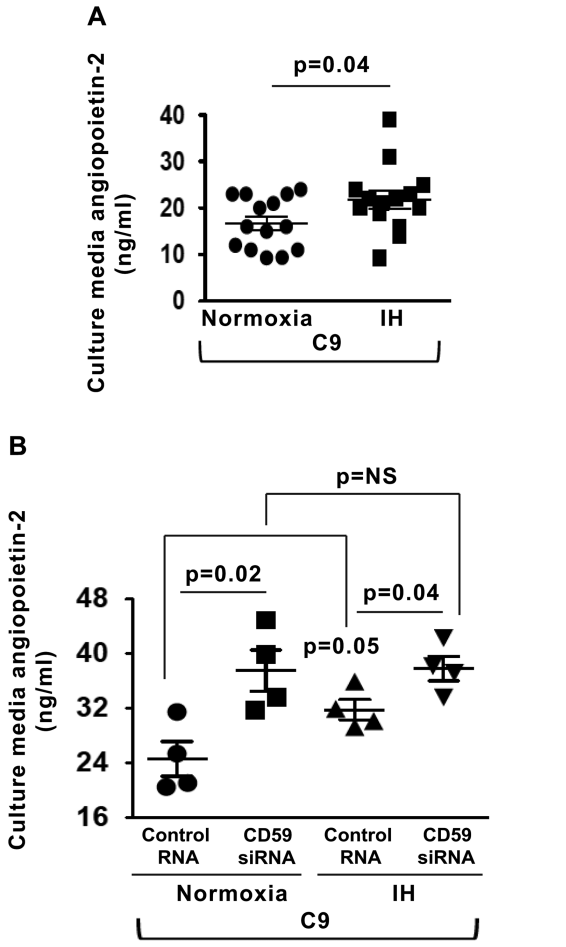

Figure 4. IH enhances complement-mediated release of endothelial angiopoietin-2. (A) Quantitation of angiopoietin-2 levels in HUVEC culture media after stimulation with recombinant C9 in normoxia and IH expressed in ng/mL (n = 14). (B) Quantitation of angiopoietin-2 levels in HUVECs culture media in normoxia and IH after stimulation with C9 and transfection with CD59 siRNA or control RNA expressed in ng/mL (n = 4). All data throughout the figure are shown as the mean ± SE, two-sided t-test test. Abbreviations as in Figure 2.

release of angiopoietin-2 from WPB via complement activity. Indeed, stimulation with C9 led to increased angiopoietin-2 release into the culture media in IH compared with normoxia (Figure 4, A). Silencing of CD59 resulted in significantly increased release of angiopoietin-2 in normoxia, whereas in IH, there was a minimal further increase compared with controls, suggesting that IH increases angiopoietin-2 release predominantly by promoting internalization of CD59 from the EC surface (Figure 4, B).

IH promotes interaction between CD59 and WPB in OSA

We next assessed whether intracellular CD59 interacts with WPB in ECs harvested from OSA patients and controls. Using Duolink (in situ proximity ligation assay) and vWF as a marker for WPB, we detected CD59-WPB interaction in ECs harvested from healthy controls, indicating the proximity of CD59 to WPB in healthy individuals (Figure 5, A) [16, 23]. In ECs harvested from OSA patients, the co-localization of intracellular CD59 and vWF was increased compared with controls (Figure 5, B), suggesting that OSA enhances interactions between intracellular CD59 and WPB. Co-localization of intracellular CD59 and vWF did not correlate with AHI and was not significantly associated with age, gender, BMI, SBP, or DBP (Table S6).

To investigate whether IH, a hallmark of OSA, mediates interactions between WPB and intracellular CD59 in ECs, we used an in vitro model of IH [5]. Similar to OSA patients, IH increased co-localization of intracellular CD59 and vWF in HUVECs (Figure 6, A and B). Total cellular levels of CD59 protein were similar in ECs exposed to normoxia or IH (mean ± SE, 100 ± 2.0 vs. 95 ± 3.4 respectively, p = NS), suggesting that increased co-localization of intracellular CD59 with WPB in IH is due to the enhanced internalization of CD59 from the plasma membrane rather than upregulation of the protein expression.

To investigate whether CD59 interacts directly with vWF, we performed co-immunoprecipitation (CO-IP) using HUVECs whole cell lysate incubated with beads coated with anti-vWF antibodies. No CD59 protein was detected in the ensuing immunoprecipitate despite an abundant amount of CD59 in the starting lysate (Figure 6, C), suggesting that vWF does not interact directly with CD59.

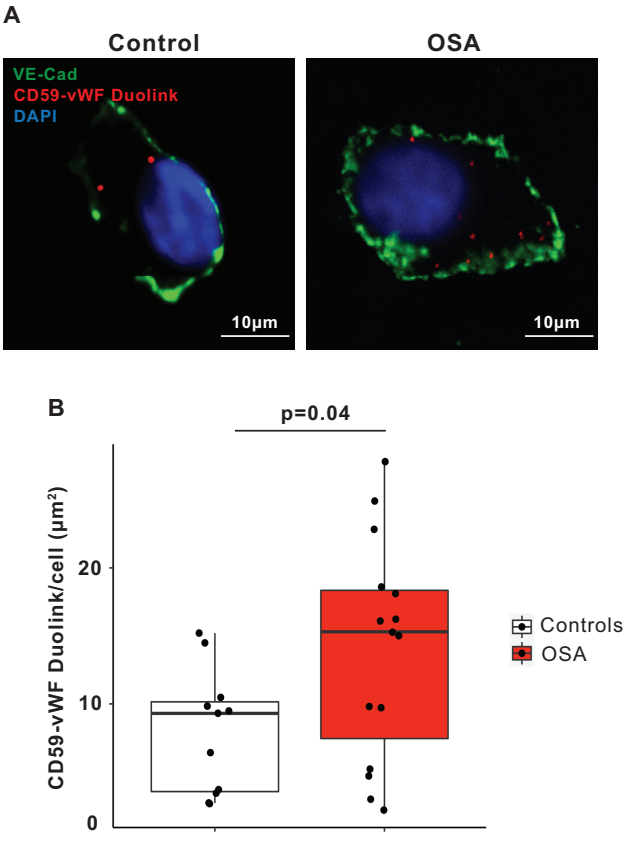

Figure 5. OSA promotes co-localization of intracellular CD59 with WPB in ECs. (A) Representative confocal images of DuoLink signal between CD59 and Weibel-Palade Body (WPB) in ECs harvested from obstructive sleep apnea (OSA) patient and control. EC plasma membrane is identified by immunofluorescence for vascular endothelial (VE)–cadherin. Scale bar: 10 µm. (B) Quantitation of DuoLink signal in OSA patients (n = 15) and controls (n = 11) (mean ± SD, permutation test).

We then investigated whether intracellular CD59 interacts with WPB exocytosis machinery and whether IH modulated this interaction. We focused on syntaxin-3, and VAMP 3 and 8—established components of the soluble *N*-ethylmaleimide-sensitive factor attachment protein receptor (SNARE) that mediate WPB exocytosis in ECs [24]. Immunoprecipitation with beads coated with anti-syntaxin-3, anti-VAMP 3 or 8 antibodies was then performed, followed by SDS PAGE and Western blotting with anti-CD59 in the immunoprecipitates. This identified specific binding of CD59 to syntaxin-3 (Figure 6, D) but not to VAMP 3 or VAMP 8 (Supplementary material Figure S5), suggesting that CD59 interacts directly with WPB exocytosis machinery. Remarkably, binding of intracellular CD59 to syntaxin-3 was observed in IH and was absent in normoxia (Figure 6, D), suggesting that IH promotes interaction between internalized complement inhibitor CD59 and WPB exocytosis machinery.

Binding of syntaxin-3 to voltage-sensitive calcium channel $Ca_v2.3$ inhibits its opening and prevents calcium influx that is needed for exocytosis of insulin secretory granules from pancreatic β-cells, which are analogous secretory granules to WPB in ECs [25]. ECs express voltage-sensitive calcium channels $Ca_v1.2$ and $Ca_v3.1$ [26]. We detected $Ca_v1.2$ but not $Ca_v3.1$ in HUVECs lysate (Figure 6, E). We investigated whether $Ca_v1.2$ interacts with syntaxin-3 and whether IH alters such interactions. In normoxia, $Ca_v1.2$ bound to syntaxin-3 whereas IH markedly attenuated this interaction (Figure 6, E). These data suggest that IH promotes the association of syntaxin-3 with CD59 and dissociation from $Ca_v1.2$, which may attenuate the inhibitory effect of syntaxin-3 on $Ca_v1.2$ and lead to calcium influx that is needed for exocytosis of secretory granules [9, 25].

Cytosolic calcium increase resulting from calcium influx across plasma membrane plays a key role in MAC-dependent vWF secretion in ECs [9]. C9 complement component, by inserting into the plasma membrane and forming a pore-like structure, provokes a similar pattern of intracellular calcium oscillation as MAC-induced pores [21]. To investigate whether calcium flux underlies complement-induced release of vWF from WPB in IH, we incubated HUVECs with C9 and cell-permeable, selective intracellular calcium chelator 1,2-bis(2-aminophenoxy) ethane-*N*,*N*,*N*′,*N*′-tetraacetic acid tetrakis (acetoxymethyl ester) (BAPTA-AM). As predicted, IH-enhanced C9-stimulated release of intracellular vWF was blocked in BAPTA-treated compared with vehicle-treated cells (Supplementary material Figure S6A–C). In addition, calcium chelation abolished increased expression of vWF on the EC surface in IH (Supplementary material Figure S6D and E), suggesting that complement-induced vWF release from WPB in IH is calcium-dependent. Similarly, calcium chelation blocked angiopoietin-2 release from WPB (Supplementary material Figure S6F). Taken together, these data suggest that complement-induced WPB exocytosis in IH is calcium-dependent.

Statin reduces IH-induced endothelial vWF and angiopoietin-2 release.

Considering that the impaired complement inhibition stimulates vWF and angiopoietin-2 release in IH, we investigated whether stabilizing CD59 on the EC surface may exert a protective effect against vWF and angiopoietin-2 release in IH. We have previously shown that statin, an inhibitor of 3-hydroxy-3-methylglutaryl-CoA reductase, retains CD59 at the EC surface thereby exerting a protective effect against IH-induced MAC deposition [5]. We investigated whether statin treatment affects complement-dependent vWF and angiopoietin-2 release in IH. HUVECs were pretreated with atorvastatin or vehicle for 16 h followed by exposure to normoxia or IH and incubation with C9. Compared with vehicle, treatment with atorvastatin reduced the release of vWF from WPB in IH as evidenced by increased intracellular expression of vWF protein and its reduced concentration in the culture media (Figure 7, A–C). As expected, expression of vWF on the EC surface was greater in IH compared with normoxia in vehicle-treated cells (Figure 7, D). In contrast, in atorvastatin-treated cells, expression of vWF on the EC surface was similar in IH and normoxia (Figure 7, E). Similarly, atorvastatin reduced the release of angiopoietin-2 from WPB in IH (Figure 7, F), suggesting that atorvastatin inhibits complement-dependent secretion of vWF and angiopoietin-2 triggered by IH.

Discussion

The novel findings of this study are that IH promotes complement-mediated exocytosis of WPB in ECs leading to the release of vWF, a pro-thrombotic multimer, and angiopoietin-2, a pro-inflammatory cytokine that destabilizes endothelial barrier, in OSA patients. Restoring endothelial complement

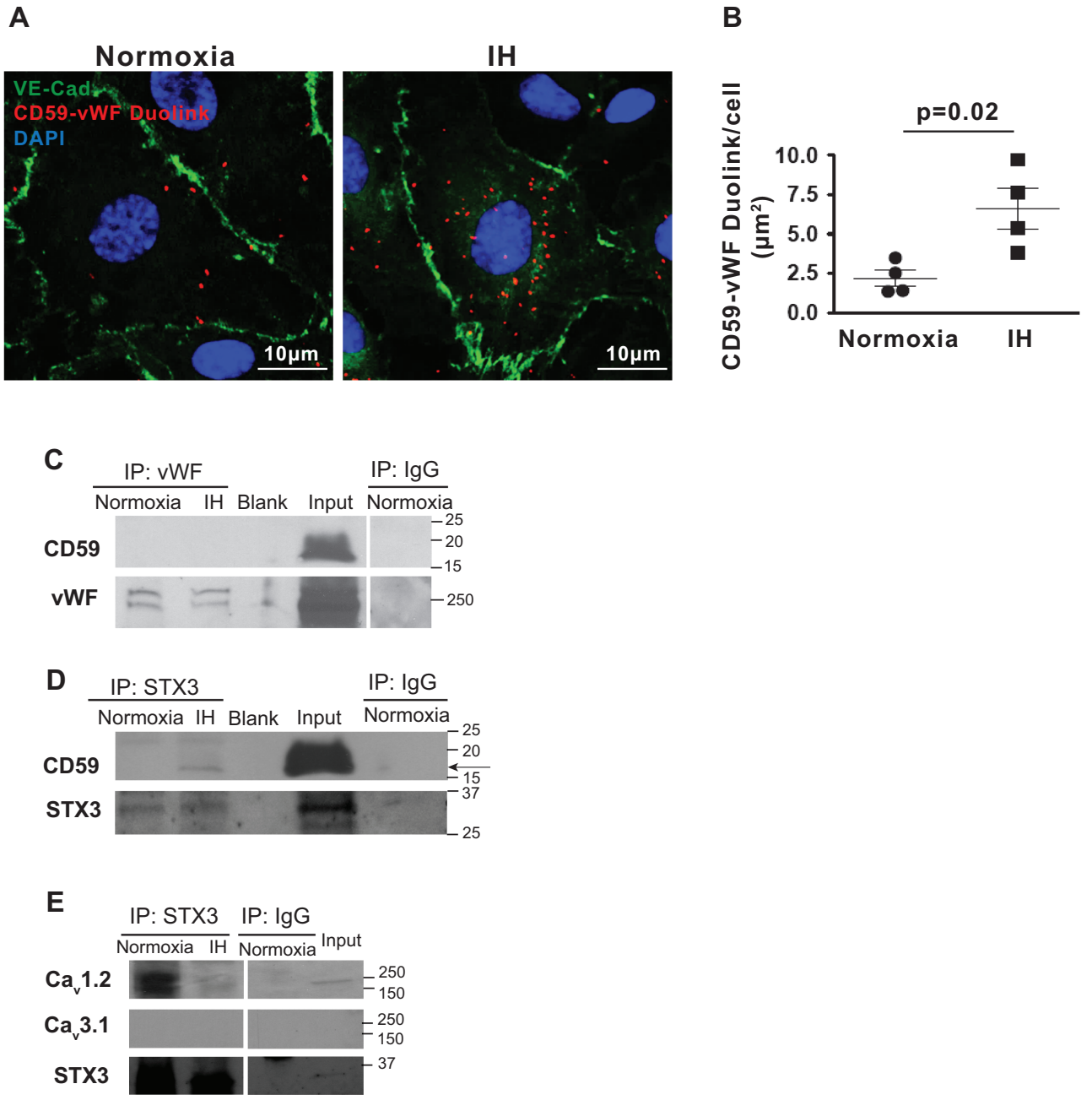

Figure 6. IH promotes co-localization of intracellular CD59 with WPB in ECs. (A) Representative confocal images of DuoLink signal between CD59 and Weibel-Palade Body (WPB) in HUVECs in normoxia and IH. EC plasma membrane is identified by immunofluorescence for VE–cadherin. Scale bar: 10 μm. (B) Quantitation of DuoLink signal in normoxia and IH (n = 4). (C) Western blot probed with antibodies directed against CD59 and vWF in the immunoprecipitate of vWF in HUVECs exposed to normoxia and IH. (D) Western blot probed with antibodies directed against CD59 and STX3 in the immunoprecipitate of STX3 in HUVECs exposed to normoxia and IH. The experiment was reproduced three times. (E) Western blot probed with antibodies directed against $Ca_v1.2$, $Ca_v3.1$, and STX3 in the immunoprecipitate of STX3 in HUVECs exposed to normoxia and IH. IgG served as negative control in (C), (D), and (E). Data in B are shown as the mean ± SE, two-sided t-test. $Ca_v1.2$, Voltage-sensitive Calcium Channel L-type 1.2; $Ca_v3.1$, Voltage-sensitive Calcium Channel T-type 3.1; STX3, Syntaxin-3. Other abbreviations as in Figure 2.

inhibition by stabilizing the cell surface expression of CD59 with statins reduced IH-mediated exocytosis of WPB. These findings establish pro-thrombotic consequences of impaired endothelial complement inhibition in IH and suggest that statin therapy may stabilize endothelial barrier and reduce pro-thrombotic condition associated with OSA.

Complement activation promotes the rapid release of vWF from WPB via calcium influx through plasma membrane pores that form after MAC deposition to ECs [9–11]. In OSA patients, IH reduces endothelial protection against complement by promoting internalization of a complement inhibitor CD59 from the EC surface, which leads to increased MAC deposition to ECs [5]. The resulting endothelial injury can compromise vascular integrity and trigger thrombus formation, both of which drive the progression of a vascular thromboembolic disease that is strongly associated with OSA [2, 27]. We found that intracellular CD59 shows markedly increased co-localization with WPB, secretory granules that store vWF

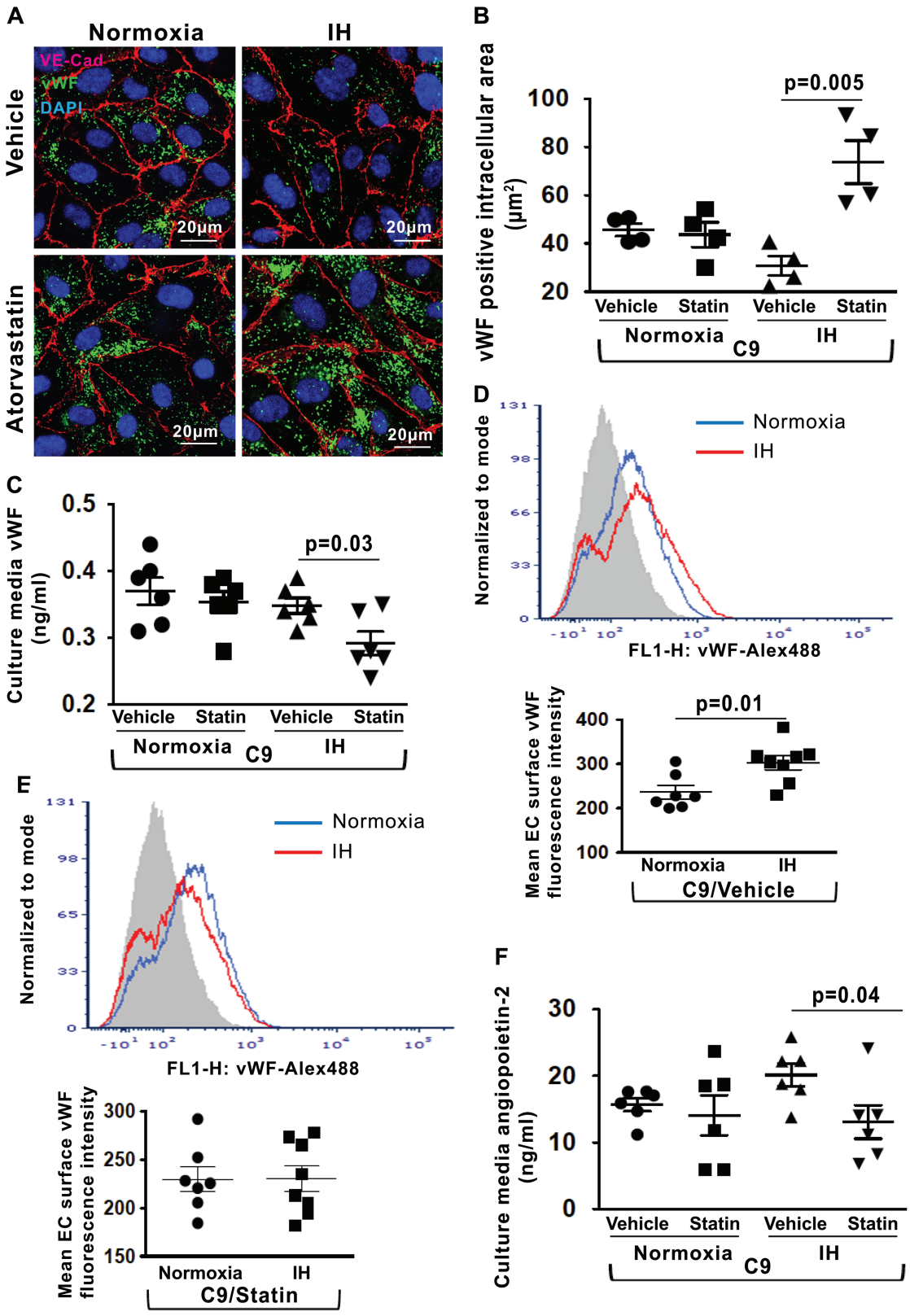

Figure 7. Statin reduces IH-induced endothelial vWF and angiopoietin-2 release. (A) Representative confocal images of intracellular vWF protein expression in HUVECs after stimulation with recombinant C9 and treatment with atorvastatin or vehicle in normoxia and IH. EC plasma membrane is identified by immunofluorescence for VE–cadherin. Scale bars: 20 μm. (B) Quantitation of intracellular vWF protein expression (fluorescence area in μm²) in HUVECs after stimulation with C9 and treatment with atorvastatin or vehicle in normoxia and IH ($n = 4$). (C) Quantitation of vWF levels in HUVECs culture media in normoxia and IH after stimulation with C9 and treatment with atorvastatin or vehicle ($n = 6$). (D) Representative histogram with a log scale x-axis and quantification of vWF fluorescence intensity on the cell surface in HUVECs in normoxia ($n = 7$) and IH ($n = 8$) after stimulation with C9 and treatment with vehicle. (E) Representative histogram with a log scale x-axis and quantification of vWF fluorescence intensity on the cell surface in HUVECs in normoxia ($n = 7$) and IH ($n = 8$) after stimulation with C9 and treatment with atorvastatin. (F) Quantitation of angiopoietin-2 levels in HUVECs culture media in normoxia and IH after stimulation with C9 and treatment with atorvastatin or vehicle expressed in ng/mL ($n = 6$). All data throughout the figure are shown as the mean ± SE, two-sided *t*-test test. Abbreviations as in Figure 2.

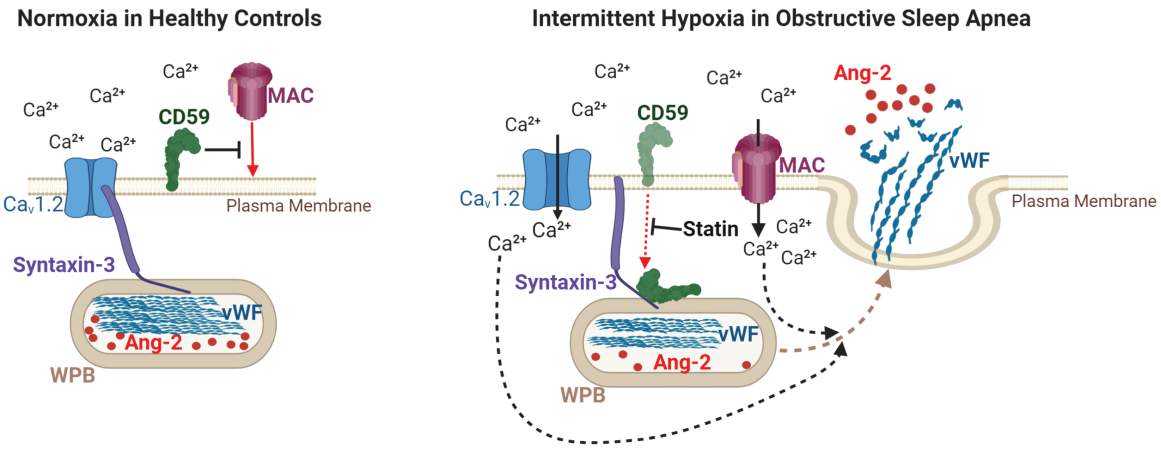

Figure 8. Mechanisms mediating endothelial von Willebrand Factor and angiopoietin-2 release in OSA. Intermittent hypoxia (IH), a hallmark of obstructive sleep apnea (OSA), reduces endothelial protection against complement by reducing expression of complement inhibitor CD59 on the endothelial cell surface, which leads to increased formation and deposition of terminal complement membrane attack complex (MAC) on the cell surface. MAC promotes calcium influx resulting in increased intracellular calcium level, which enhances the releases of von Willebrand factor (vWF) and angiopoietin-2 (Ang-2) from their storage granules Weibel-Palade bodies (WPB). WPB exocytosis in IH is further augmented by binding of intracellular CD59 to syntaxin-3—a part of WPB exocytosis machinery, which leads to dissociation of syntaxin-3 from calcium channel $Ca_v1.2$ and further calcium influx. Statin stabilizes CD59 on the endothelial cell surface, and thus protects endothelium from MAC attack, which prevents release of vWF and angiopoietin-2 from WPB and may reduce pro-thrombotic and pro-inflammatory conditions in OSA.

and angiopoietin-2, in OSA patients. In cultured ECs, we identified syntaxin-3, a part of WPB exocytosis machinery, as a binding site for intracellular CD59 on WPB in IH. In contrast to normoxia where no interaction between CD59 and syntaxin-3 was detectable, IH induced binding of intracellular CD59 to syntaxin-3, suggesting that IH promotes interaction between internalized complement inhibitor CD59 and WPB exocytosis machinery. In normoxia, syntaxin-3 binds to voltage-sensitive calcium channels and inhibits calcium influx, which precludes exocytosis of secretory granules [25]. In IH, voltage-sensitive calcium channel $Ca_v1.2$ binding to syntaxin-3 was markedly attenuated compared with normoxia, suggesting that IH diminishes the inhibitory effect of syntaxin-3 on $Ca_v1.2$. Consequent calcium influx may augment calcium oscillations resulting from MAC-induced pore formation in IH, enhancing complement-mediated WPB exocytosis and the release of vWF and angiopoietin-2 in OSA [21].

Interestingly, most of the vWF released from WPB appears to be retained on the EC surface in IH in vitro model. Upon release from WPB, the high molecular weight vWF multimers are anchored at the EC surface and undergo ADAMTS13-catalyzed proteolysis in which a specific peptide bond in the vWF A2 domain is cleaved—a process facilitated by the blood flow (i.e. fluid shear force) that promotes unfolding of vWF multimer and exposure of the A2 domain [28]. In vitro, vWF may unfold less efficiently owing to the absence of fluid shear force. In addition, C9-stimulated release of vWF may outpace the constitutive release of ADAMTS13 resulting in vWF retention on the EC surface [28]. In contrast, the local shear stress facilitates the unfolding of vWF and enables its efficient cleavage in vivo [29]. The levels of circulating cleavage products of secreted vWF correlated with the severity of OSA and the degree of repetitive hypoxemia, suggesting that OSA contributes independently to vWF release. Circulating vWF multimers can adhere to exposed subendothelial matrix as well as self-associate with surface-immobilized vWF, forming hyperactive filamentous network that potently promotes platelet adhesion and initiates pro-thrombotic cascade, which may underlie pro-thrombotic conditions associated with OSA [30, 31].

In addition to vWF, WPB store angiopoietin-2, a proangiogenic factor that is upregulated in multiple inflammatory diseases and has been implicated in the direct control of inflammatory response [17]. Patients with OSA, who were free of significant comorbidities, had elevated circulating levels of angiopoietin-2 compared with controls. IH-mediated impairment in complement inhibition enhanced the release of angiopoietin-2 from WPB compared with normoxia, suggesting that IH stimulates the release of angiopoietin-2 in OSA. Upon secretion from WPB, angiopoietin-2 acts both in autocrine and paracrine manner to amplify endothelial inflammation and disturb endothelial junctional integrity [32–34]. Recently, deleterious mutations in ANGPT2, which encodes angiopoietin-2, were found to be associated with both reduced average SaO_2 levels and greater oxyhemoglobin desaturation during apneas and hypopneas in patients with OSA [18]. Lower SaO_2 levels are also associated with higher serum angiopoietin-2 levels in men [18]. Elevated angiopoietin-2 levels have been associated with increased risk for cardiovascular diseases in the Framingham Heart Study as well as all-cause and cardiovascular mortality [35, 36]. Angiopoietin-2 levels did not correlate with the severity of OSA in our study. The lack of correlation may be because most of the patients had mild to moderate OSA and were mostly free of comorbidities, except for hypertension. It is possible that OSA patients with more severe OSA and existing cardiovascular conditions may have greater circulating levels of angiopoietin-2. Nevertheless, our findings of increased angiopoietin-2 release in the setting of IH-induced impairment in complement inhibition provide the first mechanistic insight into epidemiologic observations linking circulating levels of angiopoietin-2 to the severity of IH in OSA patients.

Emerging evidence suggests that statins may protect against IH-induced vascular injury through pleiotropic actions [37–39]. Our data further support a potential role of statin in improving endothelial function. Statins suppress thrombin-stimulated

WPB exocytosis [40]. However, the mechanisms underlying this effect remain unclear. We recently discovered that statins stabilize CD59 on the EC surface by reducing its internalization in IH, which restores complement inhibition in OSA patients [5]. Stabilization of CD59 on the EC surface after treatment with atorvastatin suppressed complement-dependent angiopoietin-2 and vWF release from WPB in response to IH, suggesting that statin therapy may stabilize endothelial barrier function and reduce pro-thrombotic conditions in OSA in a CD59-dependent manner. The cellular mechanisms underlying the effects of IH and statin on vWF and angiopoietin-2 release in OSA are summarized in Figure 8.

Study limitations include the use of venous ECs, which are well suited for the investigation of the venous thromboembolic risk and less so for diseases primarily involving arterial vasculature. However, venous and arterial ECs are exposed to the same circulating pro-inflammatory factors and IH in OSA [41, 42]. Inflammatory and oxidative pathways are activated similarly in venous and arterial ECs in healthy subjects and patients with atherosclerosis [41, 42]. Another limitation is the duration of hypoxic episodes. For in vitro experiments, we used repetitive 30 min episodes of hypoxia, which differ from the duration of the hypoxic episodes in OSA patients that typically last 20–40 s. This was due to the time required to achieve the set level of hypoxia in the hypoxic chamber, which is slightly longer than the typical hypoxic episode in OSA, and to ensure sufficient exposure to IH during in vitro experiments.

In conclusion, impaired endothelial complement inhibition in IH promotes complement-mediated exocytosis of WPB. The release of pro-thrombotic vWF and pro-inflammatory angiopoietin-2 from WPB may contribute to increased cardiovascular risk in patients with OSA. Treatment with statins reversed these effects in a CD59-dependent manner in IH, suggesting a possible therapeutic strategy to reduce cardiovascular risk in OSA that may be complementary to CPAP and/or particularly useful in OSA patients who do not adhere to CPAP.

Supplementary material

Supplementary material is available at *SLEEP* online.

Acknowledgments

The work is supported by NIH/NHLBI R01HL106041 and R01HL137234 and American Heart Association 16SFRN29050000 (S.J.).

Author contributions

S.G., M.E., T.T., F.C., and R.S. performed experiments, collected, analyzed, and discussed data. K.P. and A.J. recruited study participants and analyzed and discussed data. Y.W. designed a statistical plan and performed the statistical analysis. S.J. managed and designed the study, conceived experiments, and wrote the manuscript, which was revised and approved by all authors. S.J. is the guarantor of the content of the manuscript, including the data, and analysis.

Disclosure statement

Financial disclosure: none.
Non-financial disclosure: none.

References

1. Young T, *et al*. The occurrence of sleep-disordered breathing among middle-aged adults. *N Engl J Med*. 1993;**328**(17):1230–1235.
2. Marin JM, *et al*. Association between treated and untreated obstructive sleep apnea and risk of hypertension. *JAMA*. 2012;**307**(20):2169–2176.
3. Jelic S, *et al*. Inflammation, oxidative stress, and repair capacity of the vascular endothelium in obstructive sleep apnea. *Circulation*. 2008;**117**(17):2270–2278.
4. Jelic S, *et al*. Vascular inflammation in obesity and sleep apnea. *Circulation*. 2010;**121**(8):1014–1021.
5. Emin M, *et al*. Increased internalization of complement inhibitor CD59 may contribute to endothelial inflammation in obstructive sleep apnea. *Sci Transl Med*. 2016;**8**(320):320ra1.
6. Peker Y, *et al*. Effect of positive airway pressure on cardiovascular outcomes in coronary artery disease patients with nonsleepy obstructive sleep Apnea. The RICCADSA randomized controlled trial. *Am J Respir Crit Care Med*. 2016;**194**(5):613–620.
7. McEvoy RD, *et al*.; SAVE Investigators and Coordinators. CPAP for prevention of cardiovascular events in obstructive sleep Apnea. *N Engl J Med*. 2016;**375**(10):919–931.
8. Sánchez-de-la-Torre M, *et al*. Effect of obstructive sleep apnoea and its treatment with continuous positive airway pressure on the prevalence of cardiovascular events in patients with acute coronary syndrome (ISAACC study): a randomised controlled trial. *Lancet Respir Med*. 2020;**8**:359–367.
9. Hattori R, *et al*. Complement proteins C5b-9 induce secretion of high molecular weight multimers of endothelial von Willebrand factor and translocation of granule membrane protein GMP-140 to the cell surface. *J Biol Chem*. 1989;**264**(15):9053–9060.
10. Riedl Khursigara M, *et al*. Vascular endothelial cells evade complement-mediated membrane injury via Weibel-Palade body mobilization. *J Thromb Haemost*. 2020;**18**(6):1484–1494.
11. Noone DG, *et al*. Von Willebrand factor regulates complement on endothelial cells. *Kidney Int*. 2016;**90**(1):123–134.
12. Brill A, *et al*. von Willebrand factor-mediated platelet adhesion is critical for deep vein thrombosis in mouse models. *Blood*. 2011;**117**(4):1400–1407.
13. Methia N, *et al*. Localized reduction of atherosclerosis in von Willebrand factor-deficient mice. *Blood*. 2001;**98**(5):1424–1428.
14. Theilmeier G, *et al*. Endothelial von Willebrand factor recruits platelets to atherosclerosis-prone sites in response to hypercholesterolemia. *Blood*. 2002;**99**(12):4486–4493.
15. Doddapattar P, *et al*. Endothelial cell-derived von Willebrand factor, but not platelet-derived, promotes atherosclerosis in apolipoprotein E-deficient mice. *Arterioscler Thromb Vasc Biol*. 2018;**38**(3):520–528.
16. Ewenstein BM, *et al*. Composition of the von Willebrand factor storage organelle (Weibel-Palade body) isolated from cultured human umbilical vein endothelial cells. *J Cell Biol*. 1987;**104**(5):1423–1433.
17. Scholz A, *et al*. Angiopoietin-2: a multifaceted cytokine that functions in both angiogenesis and inflammation. *Ann N Y Acad Sci*. 2015;**1347**:45–51.

18. Wang H, *et al*. Variants in angiopoietin-2 (ANGPT2) contribute to variation in nocturnal oxyhaemoglobin saturation level. *Hum Mol Genet*. 2016;**25**(23):5244–5253.
19. Kapur VK, *et al*. Clinical practice guideline for diagnostic testing for adult obstructive sleep apnea: an American academy of sleep medicine clinical practice guideline. *J Clin Sleep Med*. 2017;**13**(3):479–504.
20. O'Donnell J, *et al*. The relationship between ABO histo-blood group, factor VIII and von Willebrand factor. *Transfus Med*. 2001;**11**(4):343–351.
21. Wood A, *et al*. Specific induction of intracellular calcium oscillations by complement membrane attack on oligodendroglia. *J Neurosci*. 1993;**13**(8):3319–3332.
22. Podack ER, *et al*. Killing of microbes and cancer by the immune system with three mammalian pore-forming killer proteins. *Front Immunol*. 2016;**7**:464.
23. Gullberg M, *et al*. Duolink-"In-cell Co-IP" for visualization of protein interactions in situ. *Nat Methods*. 2011;**8**:i–ii.
24. Schillemans M, *et al*. Weibel-Palade body localized syntaxin-3 modulates von Willebrand factor secretion from endothelial cells. *Arterioscler Thromb Vasc Biol*. 2018;**38**(7):1549–1561.
25. Xie L, *et al*. Syntaxin-3 binds and regulates both R- and L-Type calcium channels in insulin-secreting INS-1 832/13 cells. *PLoS One*. 2016;**11**(2):e0147862.
26. Cheng J, *et al*. Ion channels and vascular diseases. *Arterioscler Thromb Vasc Biol*. 2019;**39**(5):e146–e156.
27. Arnulf I, *et al*. Obstructive sleep apnea and venous thromboembolism. *JAMA*. 2002;**287**(20):2655–2656.
28. Turner NA, *et al*. Endothelial cell ADAMTS-13 and VWF: production, release, and VWF string cleavage. *Blood*. 2009;**114**(24):5102–5111.
29. Huang J, *et al*. Integrin alpha(v)beta(3) on human endothelial cells binds von Willebrand factor strings under fluid shear stress. *Blood*. 2009;**113**(7):1589–1597.
30. Barg A, *et al*. Soluble plasma-derived von Willebrand factor assembles to a haemostatically active filamentous network. *Thromb Haemost*. 2007;**97**(4):514–526.
31. Savage B, *et al*. Functional self-association of von Willebrand factor during platelet adhesion under flow. *Proc Natl Acad Sci U S A*. 2002;**99**(1):425–430.
32. Maisonpierre PC, *et al*. Angiopoietin-2, a natural antagonist for Tie2 that disrupts in vivo angiogenesis. *Science*. 1997;**277**(5322):55–60.
33. Fiedler U, *et al*. The Tie-2 ligand angiopoietin-2 is stored in and rapidly released upon stimulation from endothelial cell Weibel-Palade bodies. *Blood*. 2004;**103**(11):4150–4156.
34. Scharpfenecker M, *et al*. The Tie-2 ligand angiopoietin-2 destabilizes quiescent endothelium through an internal autocrine loop mechanism. *J Cell Sci*. 2005;**118**(Pt 4):771–780.
35. Lieb W, *et al*. Clinical and genetic correlates of circulating angiopoietin-2 and soluble Tie-2 in the community. *Circ Cardiovasc Genet*. 2010;**3**(3):300–306.
36. Lorbeer R, *et al*. Circulating angiopoietin-2, its soluble receptor Tie-2, and mortality in the general population. *Eur J Heart Fail*. 2013;**15**(12):1327–1334.
37. Ayas NT, *et al*. Could adjunctive pharmacology mitigate cardiovascular consequences of obstructive sleep apnea? *Am J Respir Crit Care Med*. 2019;**200**(5):551–555.
38. Toraldo DM, *et al*. Statins may prevent atherosclerotic disease in OSA Patients without Co-Morbidities? *Curr Vasc Pharmacol*. 2017;**15**(1):5–9.
39. Joyeux-Faure M, *et al*. Response to statin therapy in obstructive sleep apnea syndrome: a multicenter randomized controlled trial. *Mediators Inflamm*. 2014;**2014**:423120.
40. Yamakuchi M, *et al*. HMG-CoA reductase inhibitors inhibit endothelial exocytosis and decrease myocardial infarct size. *Circ Res*. 2005;**96**(11):1185–1192.
41. Silver AE, *et al*. Overweight and obese humans demonstrate increased vascular endothelial NAD(P)H oxidase-p47(phox) expression and evidence of endothelial oxidative stress. *Circulation*. 2007;**115**(5):627–637.
42. Antoniades C, *et al*. 5-methyltetrahydrofolate rapidly improves endothelial function and decreases superoxide production in human vessels: effects on vascular tetrahydrobiopterin availability and endothelial nitric oxide synthase coupling. *Circulation*. 2006;**114**(11):1193–1201.